Bioconjugate Chemistry

Article

pubs.acs.org/bc

Insight into DNA Minor Groove Unspecific Binding of Pyrrole Polyamide

Hongwei Qiao,[†] Chunying Ma,[‡] Xiao Zhang,[‡] Xi Jing,[‡] Chao Li,*[,‡] and Yufen Zhao*[,†]

[†]Key Laboratory of Bioorganic Phosphorus Chemistry and Chemical Biology (Ministry of Education), Department of Chemistry of Tsinghua University, Beijing 100084, P. R. China

[‡]State Key Laboratory of Chemical Resource Engineering, Beijing University of Chemical Technology, 100029 Beijing, P. R. China

ABSTRACT: Chemistry-based approaches have exploited base-pairing for sequence-specific recognition of DNA. A variety of sequence-specific Py-Im hairpin polyamides to target sequences of biological interest have been widely developed. Here we reported that an eight-ring *N*-methylpyrrole polyamide can induce a strong negative signal when it interacted with ct-DNA in the minor groove, which differs from the typical CD signal induced by hairpin polyamide reported previously. Our current efforts mainly focused on investigating possible reasons and binding mode by CD spectroscopy, singular value decomposition, and atomic force microscopy. The results suggested that partly compacted DNA may form due to the unfolded binding mode that made DNA shrink along the axis of duplex. In addition, this unfolded binding was remarkably restrained in high ionic strength medium where the neutralized phosphate groups in the DNA backbone narrowed the minor groove. The present work might help to understand deeply how the Py-Im polyamides bind to duplex DNA under different conditions and, in particular, be applied to gene manipulation and expression.

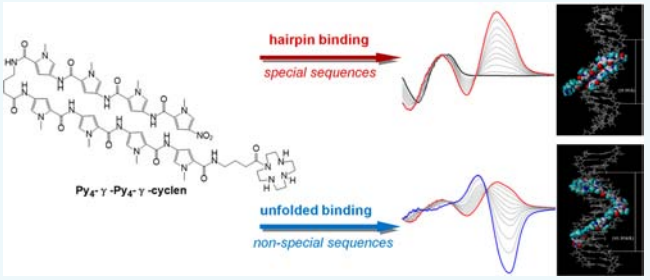

INTRODUCTION

Earlier strategies for gene targeting have been based mainly on major groove binding (triplex) or on duplex formation by strand displacement (such as by PNA).[1,2] Pyrrole-imidazole polyamides (PAs) were invented by Peter Dervan and co-workers with the aim of designing nucleo-base-pair specific agents recognizing gene targets via binding in the minor groove of double-stranded DNA, with affinity comparable to DNA binding proteins.[3−5] Here, hairpin polyamides are particularly interesting, which consist of two chains of heterocyclic amides, linked by a four-amino-butyric acid group (γ), allowing the molecule to fold back upon itself with two planar, aromatic ring systems stacked side-by-side in an antiparallel orientation within the minor groove.[6,7] Several research groups reported the structural modifications of the pyrrole and imidazole hairpin by use of other heteroaromatic compounds or fluorophores in order to improve the affinity and sequence specificity to DNA duplexes or serve as potential fluorescent DNA-binding probes.[8−14]

Circular dichroism spectropolarimetry was a powerful tool to detect and characterize DNA secondary structures changes with interaction of binding molecules.[15,16] Positive ellipticity at 300−360 nm as typical minor groove binding signals induced by polyamides has been widely reported.[17−19] Our previous work focused on the modification of less reactive DNA cleavage molecules by Py-Im polyamide, aimed at the enhancement of the double-strand cleavage selectivity.[20−22] Recently, we synthesized an eight pyrrole-containing polyamide appended with cyclen moiety (**Py_4-γ-Py_4-γ-cyclen**, Scheme 1), and expected to improve specific DNA cleavage ablility in the presence of metal ions. Interestingly, titration experiments of the polyamide into a solution of ct-DNA presented a group of unusual CD induced signals, which differed from a well-known increasing positive absorption around 335 nm. Instead, further signal changes in the minor groove binding region were observed with increase of the polyamide molecules, including the presence of both dramatic negative band and blue shift. The signal inversion could be partially attributed to different binding modes, though the details of the intricate modes and the quantitative binding constants are yet to be clarified.

In this study, the polyamide **Py_4-γ-Py_4-γ-cyclen** was investigated using CD spectroscopy and singular value decomposition (SVD) to characterize the binding geometry of the complex with large DNA (calf thymus DNA and alternative purine−pyrimidine sequences). It is important to further characterize the DNA binding modes of the polyamide to understand the basis of their nucleo-base specificity and potential interference with the expression of the targeted genes through binding in the minor groove of DNA. Investigating the effect of ionic strength could also be of interest for assessing the transformation of binding modes. Here, a four pyrrole-containing polyamide (Scheme 1) as minor groove binder

Received: June 3, 2015
Revised: August 12, 2015
Published: August 24, 2015

DOI: 10.1021/acs.bioconjchem.5b00309
Bioconjugate Chem. 2015, 26, 2054−2061

Scheme 1. Structures of Polyamide Py_4-γ-cyclen and Py_4-γ-Py_4-γ-cyclen

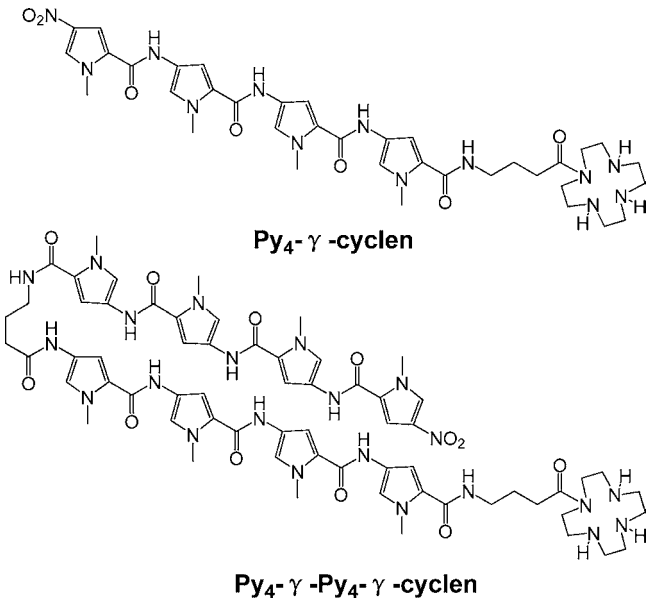

was considered relevant to include for comparison, and also because this molecule is known to exhibit the normal CD induced signals and binding mode in previous work.[20]

RESULTS

Binding of Py_4-γ-cyclen and Py_4-γ-Py_4-γ-cyclen to Calf Thymus DNA. Figure 1A shows the CD spectra from 225 to 400 nm obtained by incremental titration at 20 °C of **Py_4-γ-cyclen** into a solution of ct-DNA. Two isoelliptic points are observed at 245 and 277 nm in the DNA-absorbing wavelength region (230−300 nm), and strong DNA-induced CD bands appear at 335 nm. These are typically the observed result when a polyamide interacts appreciably with DNA minor groove. With the titration of **Py_4-γ-cyclen**, DNA was saturated at 24 mdeg ellipticity with r of 0.36 (r = [polyamide]/[ct-$DNA_{(bp)}$]).

As a case of **Py_4-γ-Py_4-γ-cyclen** shown in Figure 1B, the similar CD signals in the same region are observed at the early stage of titration (r from 0 to 0.16). However, one can see an interesting CD signal change with further increase of the polyamide molecules (Figure 1C). At r > 0.16, the original CD-induced signal at the minor groove binding region shows a dramatic decrease with a certain quantity of blue shift, whereas it begins to increase again until r = 0.24.

Positive and negative bands are saturated with r of 0.34, emerging around 313 and 349 nm, respectively. Both molar ellipticities in the DNA-absorbing region are flattened at the end point of titration. Although the unconventional changes in the minor groove binding region have not yet, to the best of our knowledge, been reported in previous work, the well-defined isoelliptic piont at 323 nm could provide evidence that two binding modes arise in the concentration-dependent binding process.

Binding of Polyamides to Alternating Purine-Pyrimidine Sequence. The next thing we most wondered is how this polyamide will behave on special sequences under the same conditions. Then, we performed the titration experiments of **Py_4-γ-Py_4-γ-cyclen** in the presence of the purine-pyrimidine sequence. At the early ratios of Py_4-γ-Py_4-γ-cyclen/poly[dA-dT]·poly[dA-dT], the increasing signal around 335 nm and decreasing at both 245 and 263 nm can be observed, as shown in Figure 2A. With the increasing ligand concentration (r > 0.02), however, the saturated titration curve at 335 nm sharply decreased with a detectable red shift, and the positive band at 263 nm and the negative band at 245 nm continued to move closer to the baseline. At r = 0.32, the induced signals in both the DNA-absorbing and minor groove binding regions were

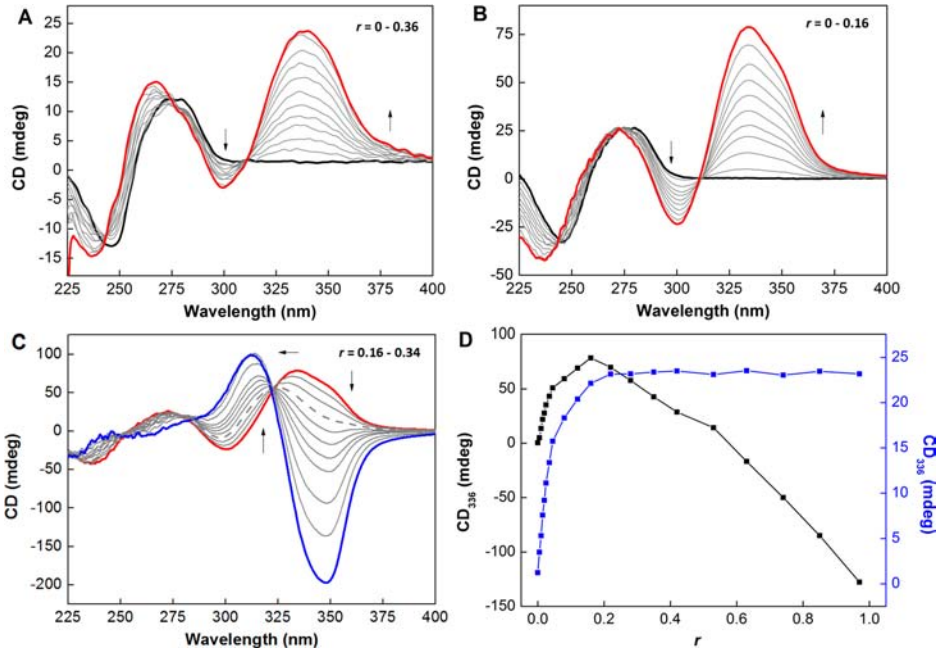

Figure 1. CD spectra of the polyamide associated with ct-DNA. (A) **Py_4-γ-cyclen**/DNA base pair ratios 0−0.36; (B) **Py_4-γ-Py_4-γ-cyclen**/DNA base pair ratios 0−0.16; (C) **Py_4-γ-Py_4-γ-cyclen**/DNA base pair ratios 0.16−0.34 (gray dashed line: r = 0.24); (D) Molar ellipticities at 335 nm for titration of **Py_4-γ-Py_4-γ-cyclen**/DNA (black ■) and **Py_4-γ-cyclen**/DNA (blue ■).

DOI: 10.1021/acs.bioconjchem.5b00309
Bioconjugate Chem. 2015, 26, 2054−2061

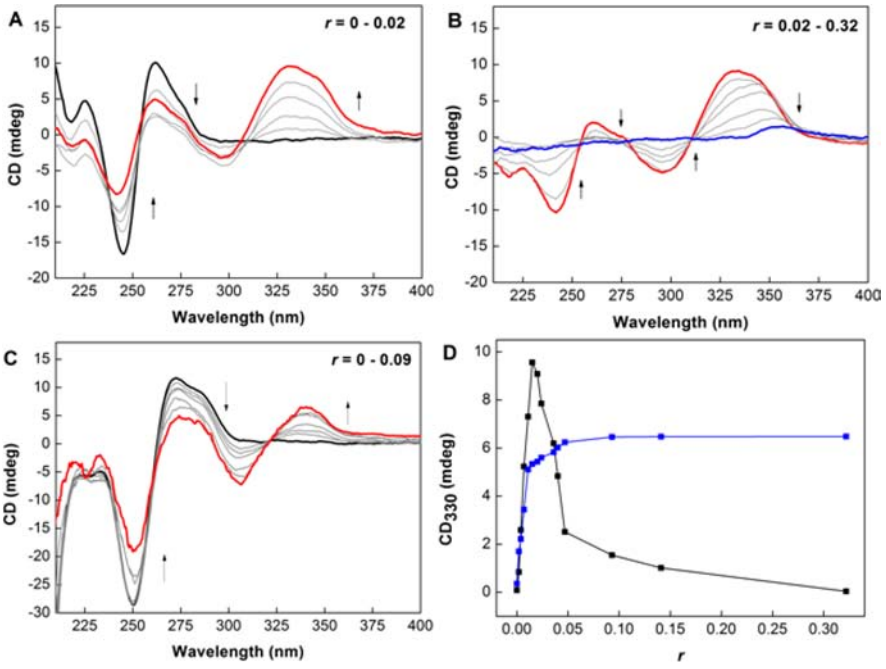

Figure 2. CD spectra of **Py_4-γ-Py_4-γ-cyclen** associated with poly[dA-dT]·poly[dA-dT] with base pair ratios of (A) 0−0.02 and (B) 0.02−0.32; and (C) poly[dC-dG]·poly[dC-dG] with base pair ratios of 0−0.09. (D) Molar ellipticities at 330 nm for titration of **Py_4-γ-Py_4-γ-cyclen** to poly[dA-dT]·poly[dA-dT] (■) and poly[dC-dG]·poly[dC-dG] (blue ■).

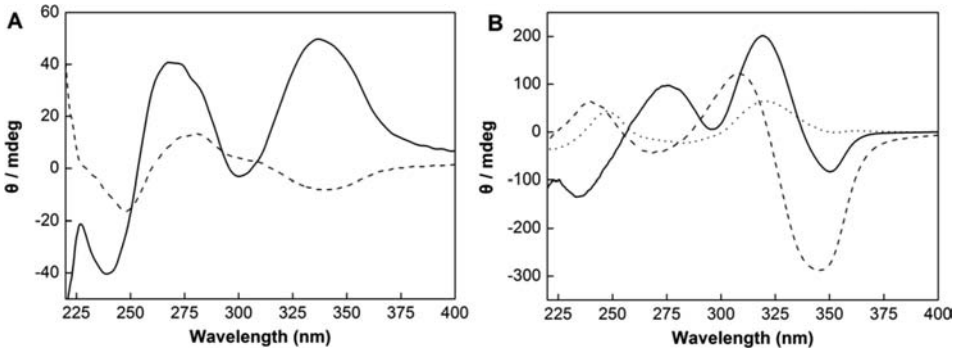

Figure 3. Basis spectra produced by SVD analysis of (A) **Py_4-γ-cyclen** and (B) **Py_4-γ-Py_4-γ-cyclen** titritions that shown in Figure 1. The most significant basis spectra, as judged by the magnitude of the singular values, correpond to spectral intensity.

almost flattened (Figure 2B). Subsequently, in the case of poly[dC-dG]·poly[dC-dG] small-scale signal changes were detected under similar titration, corresponding to an increase at 340 nm as well as decreases at both 250 and 275 nm (Figure 2C). The small spectral change implied different binding affinities to alternating purine-pyrimidine sequence. **Py_4-γ-Py_4-γ-cyclen** possessed A-T rich sequence preference, whereas binding with poly[dC-dG]·poly[dC-dG] could be attributed to simple electrostatic interactions.

Although no inversed CD signal was observed in the minor groove binding region with the increase of ligand/poly[dA-dT]·poly[dA-dT], the flattened ellipticities also indicated the polyamide bound to DNA with an unusual mode that could differ from a normal "hairpin" one.

CD Results by SVD Analysis. To quantify characteristics of the collected CD spectra, SVD was employed. The experimental CD spectra were treated as a set of vectors, and SVD was used to find an orthogonal set of "subspectra" that could be linearly combined to construct the original set of spectra. The linear coefficients were given as singular values (σ_i). The σ_i and the autocorrelations collected from CD spectra of **Py_4-γ-cyclen**/ct-DNA clearly showed that the first two components predominantly contributed to the origianl spectra shown in Figure 3A and Table 1, suggesting that only one binding mode was observed in ct-DNA. For **Py_4-γ-Py_4-γ-cyclen**, the tertiary species (σ_3) was present even at low ligand/DNA bp molar ratios, with a larger contribution to the binding

Table 1. Results of SVD analysis

	Py_4-γ-Py_4-γ-cyclen/ct-DNA		Py_4-γ-cyclen/ct-DNA	
Order	Singular V.[a]	Correlation[b]	Singular V.	Correlation
1	6014	0.938	1190	0.886
2	4799	0.809	307	0.793
3	1306	−0.788	19	−0.342
4	389	0.085	15	0.298
5	354	0.202	12	0.174
6	121	0.057	11	0.019

[a]Singular value from S matrix. [b]Autocorrelation from V matrix.

DOI: 10.1021/acs.bioconjchem.5b00309
Bioconjugate Chem. 2015, 26, 2054−2061

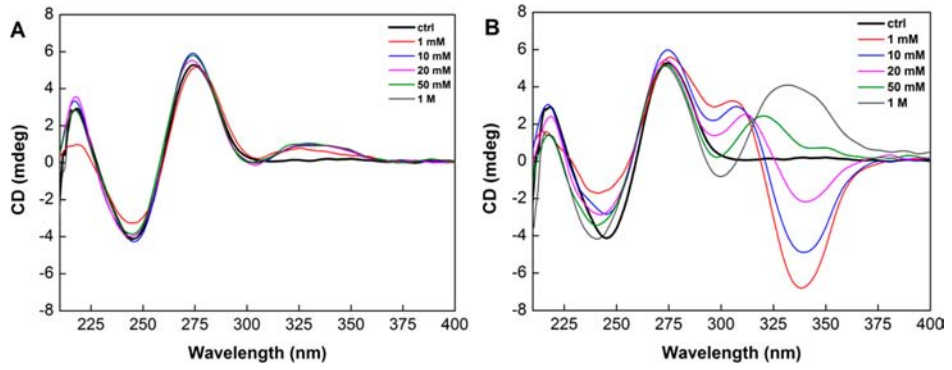

Figure 4. CD spectra of the **Py_4-γ-Py_4-γ-cyclen** /ct-DNA depending on ionic strengths with ratios of (A) 0.16 and (B) 0.34 in sodium phosphate buffer pH 7.4 at 25 °C.

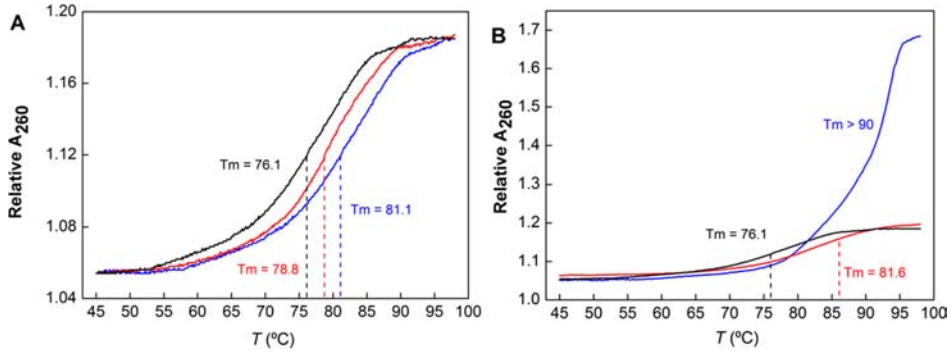

Figure 5. UV melting profiles at 260 nm for ct-DNA interacted with **Py_4-γ-cyclen** (A) and **Py_4-γ-Py_4-γ-cyclen** (B) at the ratio of 0 (black —), 0.16 (red —), and 0.34 (blue —).

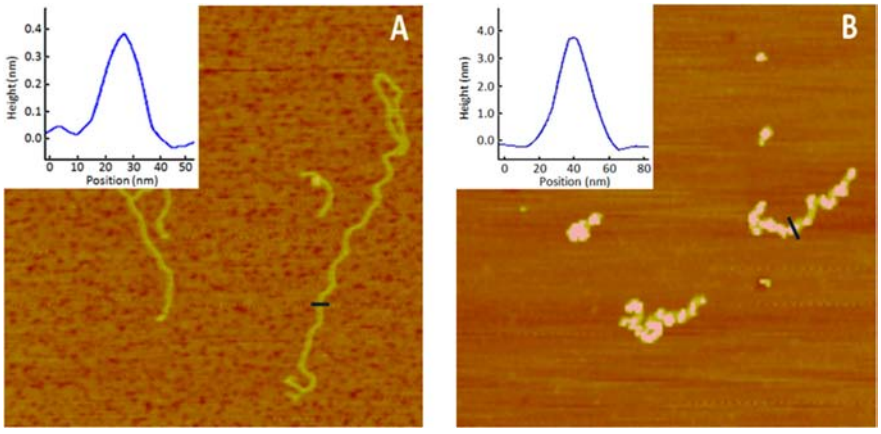

Figure 6. AFM section analysis of free ct-DNA (A) and condensates (B) induced by **Py_4-γ-Py_4-γ-cyclen**. The scale of images is 1.25 μm × 1.25 μm.

at ratios above saturation (Figure 3B). This suggested the binding process could involve two different bound species in DNA, and were consistent with their CD spectra above. In another SVD analysis from **Py_4-γ-Py_4-γ-cyclen**/poly[dA-dT]·poly[dA-dT] titration data, we also obtained three basis spectra, but the third spectrum with far less intensity confirmed that the third component contributes little information to the data set and may be neglected (data not shown).

In Table 1, V-autocorrelations are greater than 0.7 for the first three spectral species of **Py_4-γ-Py_4-γ-cyclen**; however, a sharp drop in autocorrelation is seen for species 4, indicating that species beyond the first three do not contribute significantly to the spectral signal.[23] Typically, a large gap in the magnitude of the singular values can indicate the transition from valid components to noise components.[24] Similarly, the first two spectral species of **Py_4-γ-cyclen** contribute much information to the data set.

Effects of Ionic Strength on Binding Mode. Effect of ions in medium on the interaction between ct-DNA and **Py_4-γ-Py_4-γ-cyclen** was investigated, and the results showed that ionic strength as an effective approach can be used to modulate DNA binding mode. At the low ratio (r = 0.16) shown in Figure 4A, the CD signal in the minor groove binding region (335 nm) does not show any differences at salt concentration containing 1, 10, 20, 50, and 1000 mM sodium phosphate. Nevertheless, the significant differences in CD signal with changing ionic strength were observed at a high ratio of 0.34. At 1 mM Na^+, a negative band and a blue-shifted positive band appeared at 338

DOI: 10.1021/acs.bioconjchem.5b00309
Bioconjugate Chem. 2015, 26, 2054−2061

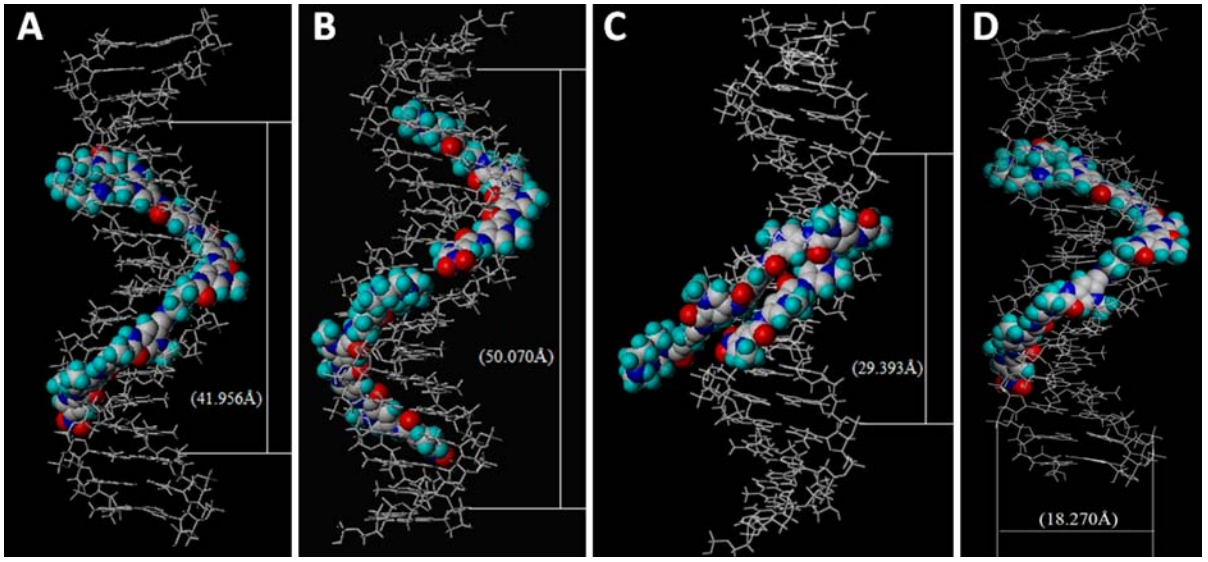

Figure 7. Schematic representation of the polyamides/DNA binding modes: (A) unfolded binding of **Py_4-γ-Py_4-γ-cyclen**; (B) sequential binding of two **Py_4-γ-cyclen**; (C) hairpin binding of **Py_4-γ-Py_4-γ-cyclen**; (D) unfolded binding of **Py_4-γ-Py_4-γ-cyclen** at high Na^+ concentration medium.

and 306 nm, respectively, suggesting a kind of probable binding mode. This is consistent with the data shown in a concentration-dependent binding process (Figure 1C). However, with the increasing ionic strength both positive and negative bands were gradually reduced; that is, the transformation from one binding mode to another was retarded. When **Py_4-γ-Py_4-γ-cyclen** binds DNA in the presence of 1 M ionic strength, only an intense positive band at 335 nm was observed as a signal characteristic of minor groove binding (Figure 4B).

T_m Measurement. UV melting experiments were conducted in the absence and presence of ligand to assess the differences, if any, between **Py_4-γ-cyclen** and **Py_4-γ-Py_4-γ-cyclen** on the thermal stabilities of the ct-DNA duplexes studied here. The resulting melting profiles are shown in Figure 5. At the ratios of 0.16 (red line) and 0.34 (blue line), **Py_4-γ-cyclen** binding increases the thermal stabilities (T_m) of ct-DNA by approximately 3 and 5 °C, respectively, as shown in Figure 5A. It is noted that a significant stabilization for the **Py_4-γ-Py_4-γ-cyclen**/ct-DNA complex with the ratio of 0.34 can be observed with T_m > 90 °C, as shown in Figure 5B. Both polyamide-induced changes in duplex thermal stability noted above are consistent with the results from CD experiments.

AFM Images. To visualize free DNA and induced by **Py_4-γ-Py_4-γ-cyclen** at nanometer resolution, AFM section analysis was performed and clearly shown in Figure 6. An image of untreated ct-DNA has been provided for comparison in Figure 6a, which shows a relaxed, linear structure with little twisting or fasciculation of the strands, presenting the characteristic ct-DNA morphology, with a height of 0.38 nm and a width of approximately 27.2 nm. In the presence of the **Py_4-γ-Py_4-γ-cyclen** (r = 0.34), the AFM image (Figure 6b) shows DNA molecules with some bulge or/and kink, presenting a number of much more compacted structures than the untreated ct-DNA, with an average height of 3.94 nm and a width of 45.4 nm. No such features were ever observed in control experiments without the polyamide. The polyamide molecule is likely to bind a DNA minor groove in the form of stretching instead of hairpin, resulting in some degree of DNA fold and compaction along the helix. In addition, structural disturbances on the binding between DNA and polyamides may lead to a kink or bump, which can be apparent or less visible depending on the viewing projection. The driving force may involve the powerful affinity between the polyamide and the corresponding bases, which could overcome base-stacking interaction. These structures are consistent with the prediction from CD spectra.

DISCUSSION

Although polyamide containing *N*-methylpyrrole and *N*-methylimidazole has been extensively studied to recognize each of the four Watson−Crick base pairs for the past decade, our present efforts attended to unspecific binding of high concentration polyamide on DNA. ct-DNA provides a model for heterogeneous DNA, representing effectively all sequence combinations. Many earlier studies have shown that the polyamide has high affinity for the duplex sequence with different binding constants depending on cognate or mismatch sequences. Generally, CD spectrometry only revealed differences in magnitudes of the induced signals with different sequences or ligand/DNA ratios. Our present results, however, showed that the positive signals in the minor groove binding region can be flipped to show the inverse ones at high ligand concentration, which could be attributed to unspecific binding mode and unhairpin molecular structure.

Long polyamides containing γ- or similar linker have been designed for specific recognition of predetermined DNA sequences with hairpin shape in the minor groove, which is strictly consistent with the Dervan pairing rules. Here we used large DNA substrate to investigate the binding mode of the "hairpin-potential" polyamide, and suspected that **Py_4-γ-Py_4-γ-cyclen** could bind to DNA minor groove with the unfolded form rather than the hairpin one, as shown in Figure 7A. On the basis of unspecific binding to large DNA, polyamide probably preferred to intercalate a minor groove in the form of unfolded molecule, and occupied a longer groove rather than a hairpin form. With the increase of ligand/DNA ratios, more space in minor groove was filled in and the overstretching ligands may partly shrink along the aixs of duplex, easily resulting in DNA compaction. The disappearing Cotton effect (Figure 1C) could correspond to a high extent of compaction

DOI: 10.1021/acs.bioconjchem.5b00309
Bioconjugate Chem. 2015, 26, 2054−2061

of complexes. Because losing intensity in both bands suggested a decrease in helicity and base-stacking of DNA,[25,26] this could be ascribed to change of DNA conformation or DNA compaction. However for eight-ring hairpin-bound ligands and two sequential-bound **Py_4-γ-cyclen**, the binding site size was reported to be 6 bp[27] and 5−6 bp, probably similar to distamycin reported, respectively, less than one DNA pitch.[28] These stable molecular conformations do not readily make compacted double-strands. A schematic model for the different modes was depicted in Figure 7B−C.

Ionic strength, one of the most critical influences on DNA binding activity, was discussed to explore if the size of the minor groove may affect the mode of binding. It is well-known that the increase of ionic strength makes the average distance narrower for DNA minor groove. This is because in a high ionic strength medium the negative charges of phosphate groups in the DNA backbone are neutralized, which resulted in the decrease of electrostatic repulsion among them. The molecular modeling showed narrower space between duplexes compared to that in lower ionic strength medium, as shown in Figure 7D. At the increasing salt concentration medium, thus, it is hard to squeeze more ligands with unfolded form into minor groove. This finding is based on the fact that the inversing CD-induced signal depended on part of the DNA compaction, and was achieved by polyamide unfolded binding mode.

CONCLUSION

The most important finding in this work is that an eight-ring *N*-methylpyrrole polyamide derivative can unspecifically bind to ct-DNA with unfolded form, and induce intense negative signal opposite to normal positive band at the minor groove binding region. SVD analysis and AFM images suggested that a DNA-compacted binding mode may arise at high ligand/DNA ratio, which was attributed to duplex shrinkage driven by unfolded polyamide. This is consistent with losing intensity in both bands, suggesting a decrease in helicity and base-stacking interaction. On the basis of this mechanism, low ionic strength was liable to cause CD induced signal inversion through DNA compaction, while high salt concentration in medium easily narrowed the minor groove, resulting in minor unfolded ligand binding to DNA. Detailed investigations into binding effect and dynamics of small DNA are still ongoing; the present results should be of value for binding behavior to large undetermined DNA, as well as a profound understanding of the polyamide binding mode as DNA minor groove binder.

MATERIALS AND METHODS

Chemistry. MS (ESI) mass spectral data were recorded on a Finnigan LCQDECA mass spectrometer. ^{1}H NMR and ^{13}C NMR spectra were measured on a Bruker AV600 spectrometer, and chemical shifts in ppm were reported relative to internal Me_4Si ($CDCl_3$). All other chemicals and reagents were obtained commercially and used without further purification. Poly[dA-dT]·poly[dA-dT] and poly[dC-dG]·poly[dC-dG] were purchased from Promega Corporation. Calf thymus DNA (ct-DNA) was purchased from Sigma (USA) Company and used as received.

Synthesis of Polyamide Derivatives. The polyamide, **Py_4-γ-cyclen** and **Py_4-γ-Py_4-γ-cyclen** (where γ is γ-aminobutyric acid), was prepared manually using protocols described elsewhere.[20] It is worth pointing out that nitro group at N-terminus is not deliberate, but becasue the same intermediate NO_2PyCOOH was used to build polyamide. The control experiment showed that the nitro group has no noticeable influence on the unique CD signals (data not shown). The polyamide was purified and analyzed using high-performance liquid chromatography (purity 95%) and ESI mass spectrometry. Stock solutions of all samples were freshly prepared in water and used within 2 days. All measurements were performed at 25 °C. **Py_4-γ-Py_4-γ-cyclen**: ^{1}H NMR (DMSO-d_6, 400 MHz), δ/ppm: 10.18 (s, 1H), 10.04 (s, 1H), 9.87 (m, 2H), 9.71 (s, 1H), 9.53 (s, 1H), 9.20 (s, 1H), 7.39 (d, 1 H, J = 1.1 Hz), 7.27 (s, 1 H), 7.20 (d, 1 H, J = 2.0 Hz), 7.18 (s, 1H), 7.13 (d, 1 H, J = 1.1 Hz), 7.12 (s, 1 H), 7.10 (d, 1 H, J = 4.1 Hz), 7.03 (d, 1 H, J = 1.4 Hz), 6.92 (m, 3 H), 6.90 (m, 3 H), 6.87 (d, 1 H, J = 2.1 Hz), 6.86 (d, 3 H, J = 2.1 Hz), 3.97 (s, 3H), 3.89 (s, 3H), 3.86−3.84 (m, 18H), 3.58 (m, 3H), 3.35 (t, 2 H, J = 4.7 Hz), 3.27 (t, 2 H, J = 3.8 Hz) 3.10 (m, 6H), 2.92 (s, 3H), 2.72 (s, 3H), 2.51 (t, 2H, J = 7.4 Hz), 2.40 (t, 2H, J = 7.7 Hz), 1.95 (t, 2H, J = 6.1 Hz), 1.91 (t, 2H, J = 6.7 Hz). ^{13}C NMR (DMSO-d_6, 100 MHz), δ/ppm: 167.5, 164.2, 161.3, 161.1, 160.4, 158.7, 157.9, 135.8, 127.6, 125.4, 124.2, 122.2, 122.7, 122.9, 121.9, 121.2, 120.3, 118.5, 117.0, 114.9, 105.8, 105.1, 104.3, 104.1, 102.9, 51.3 45.3, 42.2, 41.7, 40.4, 38.6, 35.3, 26.8, 23.5. HRMS m/z calcd for $C_{64}H_{80}N_{22}O_{12}$ $[M + H]^+$ 1349.6404; found 1349.6435.

CD Spectroscopy. Circular dichroism (CD) experiments were performed under a continuous flow of nitrogen using a Jasco-810 spectropolarimeter. A path length cell of 1 cm was used, and all experiments were performed at room temperature. A 3.3 mM stock solution of polyamide molecule was titrated into the 1.34 mg·mL^{-1} (0.134 μM, $MW_{ct\text{-}DNA} \approx 10^7$ Da) DNA solutions (pH 7.4, 10 mM sodium phosphate buffer). The standard scan parameters for all experiments used a wavelength range from 400 to 220 nm. Sensitivity was set at 100 mdeg and a scan speed of 200 nm/min. Three scans were made and computer averaged.

DNA Melting Temperature. Absorbance versus temperature profiles were measured at 260 nm using a computer-interfaced Shimadzu UV-265 spectrophotometer equipped with a thermoelectrically controlled cell holder and a cell path length of 1 cm. The heating rate in all experiments was 0.5 °C/min. For each optically detected transition, the melting temperature (T_m) was determined as described previously.[29,30] The DNA concentration was 5 μM in duplex, while the polyamide concentration ranged from 0 to 15 μM.

AFM Assay. Atomic force microscope (AFM) imaging was performed in tapping mode on a Digital Instruments multimode NanoScope III having a maximal lateral range of approximately 5 μm. All images were analyzed by tapping in air.

High-quality mica sheets (FluorMica) were cut with scissors into squares (1 cm × 1 cm) and attached with superglue to 15 mm round stainless steel sample disks (Ted Pella). Before each use, the mica was freshly cleaved by pulling off the top sheets with tape and then covered with 10 μL of autoclaved AFM buffer (10 mM Tris pH 7.5, 1 mM EDTA, 5 mM $MgCl_2$). The surface was precoated with Mg^{2+} to allow negatively charged DNA to bind. After 5 min, the buffer was rinsed thoroughly with 0.5 mL of distilled water, and the mica was briefly dried under a stream of N_2 (g).

The DNA sample was diluted with AFM buffer to 2.5 ng·μL^{-1}, and then, 10 μL of diluted sample was dropwise added to the mica surface. After 5 min, the buffer was rinsed thoroughly with 0.5 mL of distilled water, and the mica was briefly dried under a stream of N_2 (g). Each sample was

DOI: 10.1021/acs.bioconjchem.5b00309
Bioconjugate Chem. 2015, 26, 2054−2061

scanned independently three times, and three different areas were chosen in each scan.

SVD Analysis. The three-dimensional data matrix contains elements $\mathbf{A}_{i,j}$, where each row i corresponds to a concentration profile at λ_i and each column j represents a CD spectrum collected at concetration C_j. The matrix **A** was analyzed by singular value decomposition (SVD), generating three additional matrices such that $\mathbf{A} = \mathbf{USV}^T$. Matrix **S** is a diagonal matrix whose elements represent the weight of each spectral component. **U** is a matrix of basis spectra for each spectral component. **V** is a matrix of amplitude values corresponding to a spectral component's change with concentration. SVD was calculated using built-in algorithms in MATLAB v 7.11. V-vector autocorrelations (V-autocorrelations) are a measure of the apparent noise of each V-vector. The autocorrelation reflecting the signal-to-noise ratio was calculated according to

$$C(u_i) = \sum_{j=1}^{M-1} U_{j,1}U_{j+1,i} \quad (1)$$

where $U_{j,i}$ is the jth element of the ith column of matrix **U**. Because each column vector is normalized to unity, the maximum value of the autocorrelation is 1. A decrease in V-autocorrelation magnitude indicates a loss in confidence that the V-vector is significant to the spectral changes observed.

AUTHOR INFORMATION

Corresponding Authors

*E-mail: yfzhao@mail.tsinghua.edu.cn. Fax: 86 592 218 6292. Tel: 86 592 218 5610.
*E-mail: lichao@mail.buct.edu.cn. Fax: 86 10 6441 6428. Tel: 86 10 6441 3899.

Notes

The authors declare no competing financial interest.

ACKNOWLEDGMENTS

Support of this research by the National Nature Science Foundation of China is gratefully acknowledged (Nos. 21372024, 21202005, 21232005, and 21172016). Supported by "the Fundamental Research Funds for the Central Universities (No. YS1407). We thank Dr. Xin Zhang and Xinli Duan from College of Science, Beijing University and Chemical Technology, for molecular modeling. We also appreciate Jiakun Bai and Dan Chen for the synthesis of key intermediates.

REFERENCES

(1) Egholm, M., Buchardt, O., Christensen, L., Behrens, C., Freier, S. M., Driver, D. A., Berg, R. H., Kim, S. K., Norden, B., and Nielsen, P. E. (1993) PNA hybridizes to complementary oligonucleotides obeying the Watson-Crick hydrogen-bonding rules. *Nature 365*, 566−568.

(2) François, J.-C., Saison-Behmoaras, T., and Hélène, C. (1988) Sequence-specific recognition of the major groove of DNA by oligodeoxynucleotides via triple helix formation. Footprinting studies. *Nucleic Acids Res. 16*, 11431−11440.

(3) Dervan, P. B. (2001) Molecular recognition of DNA by small molecules. *Bioorg. Med. Chem. 9*, 2215−2235.

(4) Dickinson, L. A., Gulizia, R. J., Trauger, J. W., Baird, E. E., Mosier, D. E., Gottesfeld, J. M., and Dervan, P. B. (1998) Inhibition of RNA polymerase II transcription in human cells by synthetic DNA-binding ligands. *Proc. Natl. Acad. Sci. U. S. A. 95*, 12890−12895.

(5) Gottesfeld, J. M., Belitsky, J. M., Melander, C., Dervan, P. B., and Luger, K. (2002) Blocking Transcription Through a Nucleosome with Synthetic DNA Ligands. *J. Mol. Biol. 321*, 249−263.

(6) Urbach, A. R., Szewczyk, J. W., White, S., Turner, J. M., Baird, E. E., and Dervan, P. B. (1999) Sequence Selectivity of 3-Hydroxypyrrole/Pyrrole Ring Pairings in the DNA Minor Groove. *J. Am. Chem. Soc. 121*, 11621−11629.

(7) Dervan, P. B., and Edelson, B. S. (2003) Recognition of the DNA minor groove by pyrrole-imidazole polyamides. *Curr. Opin. Struct. Biol. 13*, 284−299.

(8) Takagaki, T., and Bando, T. (2012) Synthesis of Pyrrole-Imidazole Polyamide seco-1-Chloromethyl-5-hydroxy-1,2-dihydro-3H-benz[e]indole Conjugates with a Vinyl Linker Recognizing a 7 bp DNA Sequence. *J. Am. Chem. Soc. 134*, 13074−13081.

(9) Vaijayanthi, T., Bando, T., Hashiya, K., Pandian, G. N., and Sugiyama, H. (2013) Design of a new fluorescent probe: Pyrrole/imidazole hairpin polyamides with pyrene conjugation at their γ-turn. *Bioorg. Med. Chem. 21*, 852−855.

(10) Kameshima, W., Ishizuka, T., Minoshima, M., Yamamoto, M., Sugiyama, H., Xu, Y., and Komiyama, M. (2013) Conjugation of Peptide Nucleic Acid with a Pyrrole/Imidazole Polyamide to Specifically Recognize and Cleave DNA. *Angew. Chem., Int. Ed. 52*, 13681−13684.

(11) Wang, Y.-D., Dziegielewski, J., Chang, A. Y., Dervan, P. B., and Beerman, T. A. (2002) Cell-free and Cellular Activities of a DNA Sequence Selective Hairpin Polyamide-CBI Conjugate. *J. Biol. Chem. 277*, 42431−42437.

(12) Sato, A., Kawazoe, Y., Kamisuki, S., and Uesugi, M. (2006) Synthesis of synthetic small molecule transcription factors (STF). *Nucleic Acids Symp. Ser. 50*, 29−30.

(13) Sasaki, S., Bando, T., Minoshima, M., Shimizu, T., Shinohara, K.-I., Takaoka, T., and Sugiyama, H. (2006) Sequence-Specific Alkylation of Double-Strand Human Telomere Repeat Sequence by Pyrrole-Imidazole Polyamides with Indole Linkers. *J. Am. Chem. Soc. 128*, 12162−12168.

(14) Kawamoto, Y., Sasaki, A., Hashiya, K., Ide, S., Bando, T., Maeshima, K., and Sugiyama, H. (2015) Tandem trimer pyrrole-imidazole polyamide probes targeting 18 base pairs in human telomere sequences. *Chem. Sci. 6*, 2307−2312.

(15) Johnson, W. C. (2000) CD of nucleic acids. In *Circular Dichroism: Principles and Applications* (Berova, N., Nakanishi, K., Woody, R. W., Eds.) pp 703−718, Wiley-VCH, New York.

(16) Gray, D. M., Ratliff, R. L., and Vaughan, M. R. (1992) Circular dichroism spectroscopy of DNA. *Methods Enzymol. 211*, 389−406.

(17) Bhadra, K., and Kumar, G. S. (2011) Therapeutic potential of nucleic acid-binding isoquinoline alkaloids: Binding aspects and implications for drug design. *Med. Res. Rev. 31*, 821−862.

(18) Pilch, D. S., Poklar, N., Baird, E. E., Dervan, P. B., and Breslauer, K. J. (1999) The Thermodynamics of Polyamide-DNA Recognition: Hairpin Polyamide Binding in the Minor Groove of Duplex DNA. *Biochemistry 38*, 2143−2151.

(19) Chavda, S., Liu, Y., Babu, B., Davis, R., Sielaff, A., Ruprich, J., Westrate, L., Tronrud, C., Ferguson, A., Franks, A., et al. (2011) Hx, a Novel Fluorescent, Minor Groove and Sequence Specific Recognition Element: Design, Synthesis, and DNA Binding Properties of p-Anisylbenzimidazole-imidazole/pyrrole-Containing Polyamides. *Biochemistry 50*, 3127−3136.

(20) Li, C., Du, C., Tian, H., Jiang, C., Du, M., Liu, Y., Qiao, R.-Z., Jia, Y.-X., and Zhao, Y.-F. (2010) Artificial transcription factors which mediate double-strand DNA cleavage. *Chem.−Eur. J. 16*, 12935−12940 S12935/12931−S12935/12937..

(21) Li, C., Duan, S., Xu, J., Qiao, R., Xu, P., and Zhao, Y. (2012) Modulation of ascorbic acid-induced DNA cleavage by polyamide: cleavage manner, kinetics and mechanism. *Curr. Med. Chem. 19*, 921−926.

(22) Li, C., Qiao, R.-Z., Wang, Y.-Q., Zhao, Y.-F., and Zeng, R. (2008) Synthesis and biological evaluation of the Zn (II)-IDB complexes appended with oligopolyamide as potent artificial nuclease. *Bioorg. Med. Chem. Lett. 18*, 5766−5770.

(23) Shrager, R. I. (1982) Titration of individual components in a mixture with resolution of difference spectra, pKs, and redox transitions. *Anal. Chem. 54*, 1147−1152.

DOI: 10.1021/acs.bioconjchem.5b00309
Bioconjugate Chem. 2015, 26, 2054−2061

(24) Fujii, G., Chang, J. E., Coley, T., and Steere, B. (1997) The formation of amphotericin B ion channels in lipid bilayers. *Biochemistry 36*, 4959−4968.
(25) Yang, P., Wang, H., Gao, F., and Yang, B. (1996) Antitumor activity of the Cu(II)-mitoxantrone complex and its interaction with deoxyribonucleic acid. *J. Inorg. Biochem. 62*, 137−145.
(26) Clarke, M. J., Jansen, B., Marx, K. A., and Kruger, R. (1986) Biochemical effects of binding $[(H_2O)\ (NH_3)_5RuII]^{2+}$ to DNA and oxidation to[$(NH_3)_5$RuIII]n—DNA. *Inorg. Chim. Acta 124*, 13−28.
(27) Trauger, J. W., Baird, E. E., and Dervan, P. B. (1996) Recognition of DNA by designed ligands at subnanomolar concentrations. *Nature 382*, 559−561.
(28) Pelton, J. G., and Wemmer, D. E. (1989) Structural characterization of a 2:1 distamycin A.d(CGCAAATTGGC) complex by two-dimensional NMR. *Proc. Natl. Acad. Sci. U. S. A. 86*, 5723−5727.
(29) Marky, L. A., and Breslauer, K. J. (1987) Calculating thermodynamic data for transitions of any molecularity from equilibrium melting curves. *Biopolymers 26*, 1601−1620.
(30) Breslauer, K. J. (1995) Extracting thermodynamic data from equilibrium melting curves for oligonucleotide order-disorder transitions. In *Methods in Enzymology* (Johnson, M. L., Ed.) pp 221−242, Academic Press.

DOI: 10.1021/acs.bioconjchem.5b00309
Bioconjugate Chem. 2015, 26, 2054−2061